ISSN 0036-0244, Russian Journal of Physical Chemistry A, 2021, Vol. 95, No. 13, pp. 2600–2608. © Pleiades Publishing, Ltd., 2021.

PHYSICAL CHEMISTRY OF NANOCLUSTERS AND NANOMATERIALS

Preparation of Chitosan Based Polymer Microgels, Their Composites with Zinc Oxide Nanoparticles, and Physicochemical Investigation

Abbas Khan[a,*], Muhammad Rizwan[a], Luqman Ali Shah[b], Nasrullah Shah[a], Muhammad Sufaid Khan[c], Sabiha Sultana[d], and Muhammad Ismail[e]

[a] *Department of Chemistry, Abdul Wali Khan University Mardan, Mardan, 23200 Pakistan*
[b] *National Centre of Excellence in Physical Chemistry, University of Peshawar, Peshawar, 25120 Pakistan*
[c] *Department of Chemistry, University of Malakand, Chakdara, Pakistan*
[d] *Department of Chemistry, Islamia College University, Peshawar, Pakistan*
[e] *Department of Chemistry, Women University Swabi, Swabi, Pakistan*
** e-mail: abbas80@awkum.edu.pk*

Received September 8, 2020; revised November 24, 2020; accepted February 26, 2021

Abstract—The combination of inorganic nanoparticles and organic microgels can lead to the formation of novel hybrid materials with multifunctional properties; such hybrid materials reflect the properties of all of its individual components and may show synergetic effects due to the interaction between inorganic nanoparticles and microgels. Applying this concept, a new type of (zinc oxide)-poly(*N*-isopropylacrylamide)-(chitosan)-poly(acrylic acid), abbreviated as ZnO-(PNIPAAm-CS-PAA), hybrid polymer microgels were fabricated, characterized, and its physicochemical properties were studied. In the first step, the polymeric gel (PNIPAAm-CS-PAA) and ZnO particles were prepared separately. Polymer microgels were synthesized from *N*-isopropylacrylamide (NIPAM), chitosan (CS), acrylic acid (AA), and *N*,*N*'-methylene bisacrylamide (MBAm) using the free radical emulsion polymerization method. Likewise, the ZnO NPs were prepared using zinc acetate dihydrate in alcoholic medium and then centrifuged. Then, ZnO-(PNIPAAm-CS-PAA) hybrid material was prepared and purified. The hybrid materials as well as their individual components were characterized by Fourier transform infrared spectroscopy (FTIR), UV–Vis spectroscopy, scanning electron microscopy (SEM), dynamic light scattering (DLS) and thermogravimetric analysis (TGA). Presence of the absorption bands characteristic to ZnO particles in the hybrid gel samples was confirmed by both FTIR and UV–Vis spectroscopy. Similarly, differences in the surface morphology, changes in hydrodynamic diameter (D_h) of gels particles as well as in the D_h-temperature and TGA profiles of individual components compared to those of the hybrid samples provided a good proof of successful fabrication of PNIPAAm-CS-PAA microgels with nanostructured ZnO. In addition to the fundamental characterization, an overall physicochemical behavior of both pure and hybrid colloids was found to be dependent on the temperature and pH of the solution. Hence, it can be concluded that the hybrid microgel possess the combined features of incorporated components with improved stimuli-sensitive properties.

Keywords: microgels, responsive, zinc oxide, fabrication, light scattering

DOI: 10.1134/S0036024421130100

INTRODUCTION

Gels are described as three-dimensional polymers that have the properties of the liquids and solids simultaneously. Characteristically, the polymer gel swells upon absorbing good solvents (lyogel) or is a gas-filled disperse structure (aerogel); these both parts are homogeneously blended and hence the gel may be seen as the intermediate among solids and liquids or gases and solids which have an excessive range of hydrophilic clusters or regions [1, 2]. Polymer microgels are 3D cross-linked colloidal structures with the average size in their swollen state ranges from 100 nm to 5 μm. But the sizes of shrunk/collapsed shaped microgel particles are in the range of 1 to 100 nm and have colloidal properties in solution [3]. In the last two decades smart materials, such as stimuli-responsive microgels, have been the focus of many scientists due to their wide applications. The properties of microgels/hydrogels can be tuned by changing the chemical composition of the gel and conditions of the medium [4]. Some work on the physiochemical properties and stability of the copolymer gel based on *N*-isopropylamide (NIPAAm) and chitosan (CS) was reported previously [5]. Present study focuses on the nontoxic biocompatible chitosan based copolymer microgel containing chitosan (CS), *N*-isopropylamide (NIPAAm), and acrylic acid (AA). Due to the presence of temperature sensitive carbonyl group (C=O),

the temperature-sensitive monomer of microgel is NIPAAm, while the presence of AA imparts pH sensitivity to the gel. *N*,*N*-Methyene bisacrylamide (MBA) is used as a well-known cross linker due to the presence of two active double bounds. Natural biopolymers e.g., chitosan have many biological properties like biocompatibility, non-toxicity and biodegradability; due to these properties chitosan has many applications in the biomedical field [6]. Studies on CS-NIPAAm composite particle revealed that chitosan acts as a surface active agent to prevent the polymer units from clotting during the formation of the chitosan-PNIPAAm complex copolymer [7]. Likewise, Kim et al., also reported that chitosan/NIPAAm can be blended as inter-penetrating network (IPN) copolymer with variable swelling/de-swelling degree under different conditions [8].

In recent years, metal based nanoparticles have become a widely studied research topic due to their electronic, optical, mechanical, magnetic and chemical properties, which are significantly different from bulk materials. It is seen that many properties of inorganic nanoparticles can be enhanced by blending them with smart polymeric microgels. This new class of microgels, known as hybrid microgels, has been developed with loading various inorganic nanoparticles like Ag, Au, Cu, Fe_2O_3, etc., into organic based polymeric gels and studied recently for various properties and possible potential applications [9–13]. In hybrid microgel, the polymeric/organic parts maintain colloidal nature and the inorganic part imparts it many properties like photoluminescence [14], surface plasmon resonance (SPR) [15]. In targeted drugs delivery the microgels have many applications such as continuous protein release and tissue engineering, etc. [16]. Due to their good response to environment parameters such as pH and temperature, polymer gels/hybrid gels can be largely used in the biomedical field [17]. Synthesis, fundamental properties and applications of P(NIPAAm-AA) microgels were recently reviewed [18]. One of the fundamental goals of the chemists in this field is to synthesize different types of nanoparticles, microgels and their hybrid/composite material. There are still many areas in this field which need to be focused. In the present study first chitosan based PNIPAAm-CS-PAA microgel was synthesized and then ZnO NPs were prepared inside the microgel to form a new type of hybrid microgel. These organic-inorganic hybrid materials are expected to show sensitivity to external stimuli [19], therefore, they are supposed to be used for some potential applications.

Nanostructured zinc oxide (ZnO) is used as additional material in many products such as plastic, ceramics, glass, cement, lubricants, paints, ointments, batteries, ferrites, fire retardants etc. [20]. Zinc oxide is as white powder commonly known as mineral zincite. It crystallizes in three forms: hexagonal wurtzite, cubic zinc blende, and the rarely observed cubic rock salt. ZnO NPs may be used in conductive ink as an alternative to precious metals [21]. It is a versatile material having good chemical as well as physical properties. The nanostructured ZnO is chemically stable, has wide energy and beam strength [22]. From materials understanding, it is cleared that ZnO NPs are semiconductor in group II–VI, covalently located on the boundary among the covalent as well as ionic semiconductors. Because of significant piezoelectric and pyro-electric properties, ZnO NPs are used as a sensor, power producer and photo-catalyst in the production of hydrogen [23]. It is an important material for ceramics due to its hardness, inflexibility, low toxicity, bio-compatibility and bio-degradability characteristics making it an important material for biomedical usages [24].

The combination of inorganic nanoparticles and organic microgels in one hybrid system allows the preparation of new materials with multifunctional properties. However, most of the earlier literature on hybrid microgel systems is focusing on copolymer gels consisting of bi-component polymer system while tri-component copolymer gel is addressed merely in some recent reports [9, 25]. So far limited work is available on the preparation and investigation on the solution properties of (zinc oxide)-poly(*N*-isopropylacrylamide)-(chitosan)-poly(acrylic acid), abbreviated as ZnO-(PNIPAAm-CS-PAA), hybrid polymer microgels. Therefore, a full spectrum of physicochemical exploration on the stimuli-responsive behavior was carried out after successful preparation and purification of the hybrid microgel samples.

EXPERIMENTAL

Materials

Chitosan (CS, $M_w \approx 3.9 \times 10^4$ g/mol), methylene bisacrylamide (MBA), acrylic acid (AA), *N*-isopropylacrylamide (NIPAAm), ammonium persulfate (APS), zinc acetate dihydrate, methanol, 2-propanol, sodium hydroxide and acetic acid (AA) were the main materials used in this work. All these chemicals were of analytical grade and were purchased from Aldrich (Germany). Acetic acid was purchased from Cromoline (Brazil). Deionized water was obtained using a Millipore Direct-Q system.

Synthesis of PNIPAAm-CS-PAA Microgel

Free radical emulsion polymerization method was used for the synthesis of microgels containing *N*-isopropylacrylamide (NIPAAm), chitosan (CS), and acrylic acid (AA) as their main constituents [26, 27]. In these microgels *N*,*N*-methylene bisacrylamide (MBAm) was used as cross-linker and ammonium persulfate (APS) as an initiator (Table 1). In a typical polymerization experiment, NIPAAm, AA, and MBAm were added to the deionized water in a 250 mL 3-neck round bottom flask equipped with a con-

denser, nitrogen inlet and thermometer. The reaction mixture was continuously stirred, and the temperature was maintained at 70°C for 1 h while continuously supplying nitrogen gas to remove oxygen from the reaction mixture. Almost 6 mL of APS (0.06 M) was added to initiate polymerization, and the reaction was continued at 70°C for 6 h while continuously stirring and purging nitrogen. The reaction was then stopped and the microgel dispersion was cooled, centrifuged at 15 000 rpm and then taken in dialysis membrane. The prepared microgel was further purified by a 7 day dialysis through Millipore molecular porous membrane tube (cellulose membrane, MWCO 100000) at room temperature to remove unreacted monomers and other impurities by frequently changing pure water.

Synthesis of Zinc Oxide Loaded Hybrid Microgels, ZnO-(PNIPAAm-CS-PAA)

The purified microgel samples were then loaded with the as-prepared ZnO nanoparticles to get the hybrid microgels. For this purpose, ZnO nanoparticles were prepared by liquid precipitation method. Further details for the synthesis and characterization of ZnO can be seen from our previously published work [21]. The composition of various ZnO loaded hybrid gel samples is given in Table 2 while a schematic representation of its preparation scheme can be seen in Fig. 1. A very simple approach was used for the synthesis of ZnO-(PNIPAAm-CS-PAA) hybrid microgel samples [28]. Specific amount, as indicated in Table 2, of $Zn(OAc)_2{\cdot}2H_2O$ was added to 20 mL of 2-propanol and the mixture was stirred magnetically for 15 min at 20°C and then the temperature of the reaction flask was increased to 50°C and the stirring was continued for another 30 min. Afterward the reaction mixture was cooled to 15°C and the desired amount of aqueous suspension of the already prepared PNIPAAm-CS-PAA microgel was added to the reaction media and stirred for few minutes followed by dropwise addition of 1 mL of NaOH (1 M aqueous) to the reaction mixture. The reaction was allowed to continue for 30 min at 20°C and the resultant viscous milky suspension—ZnO loaded hybrid microgel was collected by centrifugation at 15000 rpm. Further purification of hybrid microgels was done by dialysis with the Millipore dialysis system (cellulose membrane, MWCO 100000). The purified samples were collected and subjected to further characterization and physicochemical investigation.

Characterization and Physicochemical Study

Basic and physicochemical characterization of the hybrid microgels and their individual constituents were carried out by Fourier transform infrared (FTIR), UV–Vis spectroscopy, scanning electron microscopy (SEM), and dynamic light scattering (DLS) techniques. FTIR analysis was performed in the wavenumber ranges from 500–4000 cm^{-1} using a Shimadzu (Japan) IR-spectrometer. A double beam, Perkin Elmer Lambda 50 UV–Vis spectrophotometer, was used to determine the UV–Vis absorption spectrum of different materials prepared. Surface morphology of the microspheres was analyzed by using of a high resolution SEM (JSM-5910, JEOL, Japan) at an accelerating voltage of 20 kV. Hydrodynamic size of the pure and hybrid gels in aqueous solutions was measured on a standard Malvern Zetasizer NANO ZS dynamic light scattering spectrometer (Malvern Instruments Limited, UK), using a He–Ne laser with a wavelength of 633 nm, and a detector angle of $\theta = 90°$. Thermogravimetric analysis (TGA) of the solid samples was conducted on thermogravimetric analyzer from Perkin Elmer, USA model Pyrin Diamond Series TG/DTA.

Table 1. Summary of the composition of pure microgel samples

Sample code	NIPAAm, mg	CS, mg	AA, mL	MBA, mg	APS (0.8 M), mL	Water, mL
RE	500	500	20	10	06	100
RG	1000	500	20	10	06	100

Table 2. Summary of the composition of ZnO loaded hybrid microgels

Sample code	$Zn(OAc)_2{\cdot}2H_2O$, g	Microgel, mL	2-Propanol, mL	NaOH, mL
REA	1.06	3	20	1
REB	1.01	5	20	1
REC	1.00	7	20	1
RED	0.66	7	20	1
RGA	1.01	3	20	1
RGB	1.00	5	20	1
RGC	1.00	7	20	1
RGD	0.66	7	20	1

RESULTS AND DISCUSSION

Fourier Transform Infrared Spectroscopy (FTIR)

Representative FTIR spectra of pure microgel (sample RG), ZnO loaded hybrid microgel (sample RGA) and ZnO NPs are shown in Fig. 2 while the spectra for other samples were almost similar qualitatively except the intensity of peaks. Various bands in the range of 500–4000 cm^{-1} were observed in the spectrum of ZnO NPs and this indicates that the surface of ZnO NPs is not bare but is stabilized with acetate groups, which originate from the starting materials and are adsorbed on the surface of nano-crystals. These moieties bounded to the surface of ZnO NPs are impurities on one side but on the other side they help in preventing the coagulation of the ZnO nanoparticles in colloidal solution [21]. Some peaks below the range of 500–1100 cm^{-1} observed in both

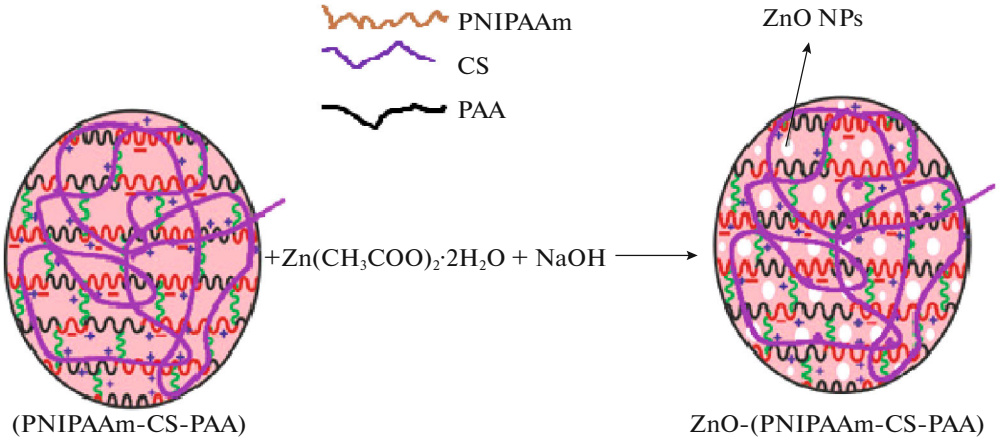

Fig. 1. Schematic representation for the preparation of the ZnO-(PNIPAAm-CS-PAA) hybrid microgels.

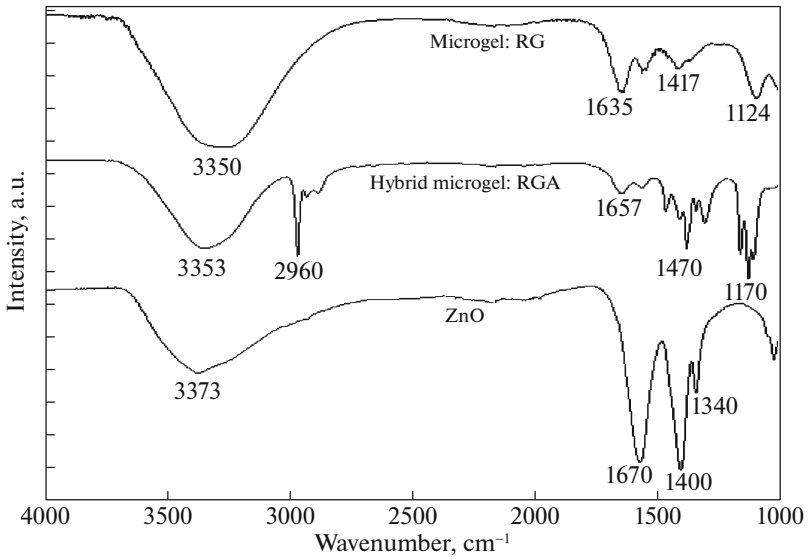

Fig. 2. Representative FTIR spectra of pure microgel (RG), ZnO loaded hybrid microgel (RGA), and ZnO NPs.

ZnO NPs and ZnO loaded hybrid gel samples, might belong to the stretching of ZnO molecule, while the peak at 1340 cm^{-1} was attributed to the symmetrical stretching of zinc acetate present as impurity on the surface of ZnO. Similarly, a peak at 1018 cm^{-1} present in ZnO and ZnO-microgel hybrid samples correspond to C–O stretching vibration of alcohol; this is possibly due to the alcohol used for dissolution of zinc acetate and ZnO nanoparticles. Another common peak arround 1400–1470 cm^{-1} observed in all samples, may be assigned to the asymmetrical stretching vibrations of acetate group of acetic acid. Relatively broader band 3350–3375 cm^{-1} is due to the O–H stretching mode of hydroxyl group. The broadness is due to the presence of adsorbed water on the surface of colloidal particles. The mentioned peaks present both in pure ZnO particles and ZnO-(PNIPAAm-CS-PAA) hybrid microgels is an indication of successful hybridization of (PNIPAAm-CS-PAA) microgels. Some of the peaks, e.g., at 2950 and 1130 cm^{-1}, were not observed in pure ZnO sample but appeared in pure as well as in hybrid microgel samples. These can be assigned to C–H stretching of methyl groups and C–N stretching of polysaccharide/chitosan/aliphatic amine, respectively, and indicated the presence of chitosan and NIPAAm in the samples. Furthermore, the typical absorption peak of –C–OH groups of both the carboxylic acid and NIPAAm are shifted to 1417 and 1470 cm^{-1} in the gel samples which is an indication of the polymerization of monomers. Spectral changes also reflect the successful fabrication of gel with ZnO [21, 27].

UV–Vis Analysis of Zinc Oxide Loaded Hybrid Microgels

UV–Vis spectroscopy is widely used for the characterization of metal based nanoparticles and hybrid materials. Especially, determination of size, shape of nanoparticles, extent of tuning of the optical and photophysical properties of both neat and hybrid materials

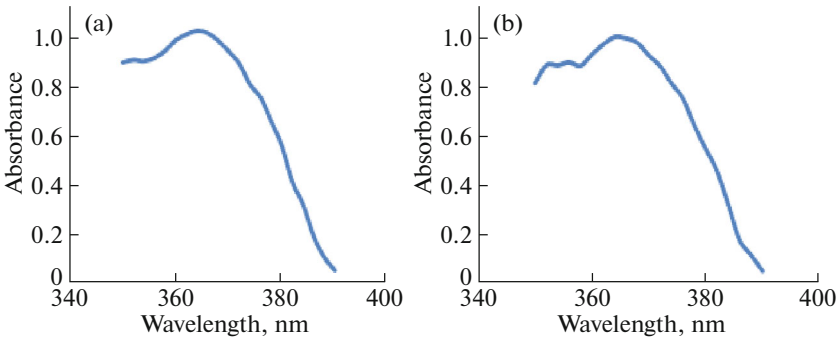

Fig. 3. Representative UV–Vis spectra of (a) pure ZnO NPs and (b) ZnO loaded hybrid microgel (RGB).

can be traced from this analytical tool [29]. Representative UV–Vis absorption spectra of pure ZnO NPs and ZnO loaded hybrid microgel samples under different experimental conditions are shown in Figs. 3–5. The spectra were measured in 70% aqueous solution of methanol as a solvent and in the range of wavelength from 350 to 400 nm at a gap of 5 nm using a double beam UV–Vis spectrometer. It can be seen that ZnO NPs strongly absorb in the UV region with a wavelength of ≈364 nm, which specifies thin particle size distribution (Fig. 3). The characteristic of metal based nanoparticles depend on the position and shape of the plasmon band. The number and location of plasmon bands are determined by the size and nature of the nanoparticles, respectively. A peak at a wavelength of 364 nm confirms the successful preparation of nanostructured ZnO colloids in the solution [21]. Figure 3 also shows a UV–Vis spectrum of a typical ZnO loaded PNIPAAm-CS-PAA hybrid microgel; it can be observed that the peaks of the zinc oxide nanoparticles in polymer microgels, appeared in range of 365–366 nm, which further support the successful fabrication of microgel with ZnO particles. A difference in the peaks of pure and hybrid ZnO particles is due to the functionalization of ZnO with polymeric gel. It is important to mention here that unlike of the hybrid gel, the original PNIPAAm-CS-PAA microgel did not give any plasmon peak in the UV–Vis spectra, which further supports the idea that successful hybridization of the gel with ZnO particles has occurred.

UV–Vis Study of Hybrid ZnO-(PNIPAAm-CS-PAA) Microgels under Changing Solution Temperature/pH

UV–Vis spectroscopic results were also used to monitor the phenomenon of swelling and de-swelling of hybrid microgels under varying temperature and pH of solution. Such results can indirectly give a clue about the growth of polymeric network around the ZnO nanoparticle core and/or the growth of ZnO nanoparticles in polymeric microgel [29]. Figure 4 shows typical UV–Vis spectra and absorbance versus pH of ZnO-(PNIPAAm-CS-PAA) hybrid microgel sample RED at different pH and at room temperature; while the results of other samples followed the same pattern and are not shown here. Figure 4 indicates that an increase in the UV–Vis absorption occurred with increasing the pH up to pH 7, while less obvious change in absorbance was observed above this pH. It further shows that change in the position of peaks is less prominent, but there is a change in the intensities and shape of the bands. This change in the shapes and absorbance of peaks occurred due to pH sensitivity of hybrid microgels due to the presence of both AA and chitosan. The prominent pH-responsive contribution is due to PAA part. However, it is important to mention here, that both chitosan and PAA chains, with $pK_a \approx 6.5$ and ≈4.75 respectively, are pH-sensitive, and that is why many physicochemical properties are changing while going from acidic pH to a basic pH region. Regular increase in absorbance of SPR band (at $\lambda = 365$ nm) with increases in pH up to 7 and then a minor increase in absorbance above this pH reflects variation in ionization capacity of the microgel at different pH of the medium. At lower pH the hybrid microgel is in the de-swollen state, while it comes to a swollen state at higher pH values. It is because that at low pH values, all the carboxylate groups are protonated, and as a result, microgel particles remain in de-swollen state. When pH of the external medium is greater than the pK_a values of chitosan ($pK_a \approx 6.5$) and PAA chains ($pK_a \approx 4.75$), the carboxylate ions are formed due to deprotonation, while $-NH_2$ groups of chitosan become $(-NH_3)^+$. Because of such ionization, these side groups developed some negative charges on the polymeric chains of the particles. Due to repulsive forces between these charged particles more spaces in the gel are created for water molecules to go inside and make the molecules more hydrophilic in nature; hence, the microgel particles swell-up and increase in size. It is proposed that strong hydrogen bonding between carboxylate ions and polar water molecules occur, which helps in holding the water molecules within the network of microgel tightly and retains it in swollen state. It is observed that the pH sensitivity of these hybrid microgels remains unchanged with loading of inorganic nanoparticles into microgel networks; however, hybridization of microgel can affect the particle size of original/pure microgel [30]. In order to check the stability of mate-

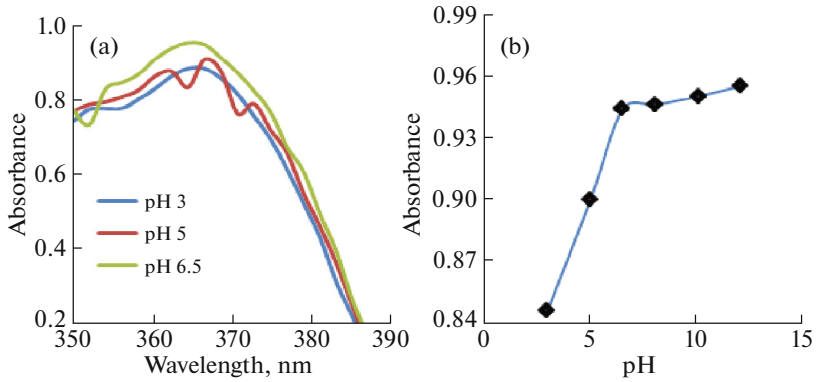

Fig. 4. Typical UV–Vis spectra (a) and absorbance versus pH (b) of ZnO-(PNIPAAm-CS-PAA) hybrid microgel sample RED at different pH and at $T = 25°C$.

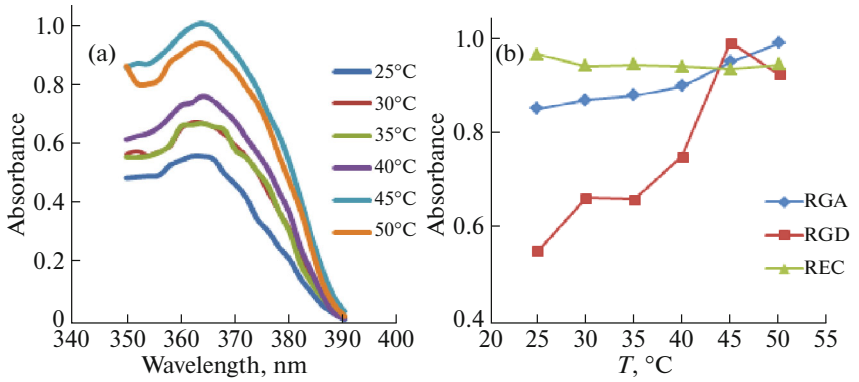

Fig. 5. Typical UV–Vis spectra for sample RGD (a) and absorbance versus temperature for three samples (b) of ZnO-(PNIPAAm-CS-PAA) hybrid microgel at different temperatures and pH 4.

rials, the ZnO loaded hybrid microgel samples were stored in aqueous solution at/near neutral pH and the UV–Vis spectra were recorded for about 3 months at an interval of one month, and no significant shift in surface plasmon band was observed, which shows good stability of the hybrid gels under neutral pH conditions.

The temperature responsive behavior of hybrid polymer microgels ZnO-(PNIPAAm-CS-PAA), due to the presence of a well-known thermo-responsive component (PNIPAAm), and their volume phase transitions was also investigated through UV–Vis spectroscopy by noting the change in absorbance at SPR at different temperatures and same pH value [31]. A plot of absorbance of colloidal dispersion versus temperature was used for finding such changes of ZnO-(PNIPAAm-CS-PAA) microgel samples as shown in Fig. 5. It is seen that an increase in absorbance occurred with temperature; this is due to the change in hydrophobic-hydrophilic interaction of colloidal particles upon variation in solution temperature. This increase in absorbance is due to an increase in the resultant size of the colloidal dispersion because of higher concentration of ZnO particles inside the microgel network.

Dynamic Light Scattering of Microgels in Dilute Solutions

Dilute aqueous colloidal solutions of pure and ZnO loaded hybrid microgels were also studied with the help of dynamic light scattering measurements (DLS). This technique gives valuable information regarding the degree of swelling, de-swelling and volume phase changes in the terms of hydrodynamic diameter as function of solution temperature and pH [27]. Representative plots of hydrodynamic diameter as a function of temperature for non-hybrid RE sample and ZnO loaded samples REA and RGA at pH 4 are given in Fig. 6. It can be seen that the hydrodynamic diameter (D_h) of gels particles as well as the D_h–temperature profiles were greatly influenced by the hybridization of microgel with ZnO particles. An increase in the size of hybrid gels (REA and RGA) compared to that of the pure gel (RE) is a clear indication of the successful and stable loading of ZnO particles into the polymeric networks of the microgel. It can be seen that hydrodynamic diameter (D_h) of gels particles regularly increasing with increase in solution temperature at constant pH, however, the slope of the graphs becomes less steeper at higher temperature ($T > 45°C$). This increase in size with temperature can be attributed to

strong interaction, in terms of H-bonding, between the side group of polymer chain and hydrated water molecules due to particles swell an overall increase in their size occurred. However, unlike our previous results on non-hybrid microgel [27], there observed no abrupt change in size of the hybrid gel samples while changing the solution temperature; this is possible due to the incorporation of ZnO particles into gel networks. These results are in good agreement with some of the earlier studies [31]. This behavior was also observed in UV–Vis spectra (Fig. 5) and in the light of this observation (matching of UV–Vis and DLS results) and our earlier results [26–28, 32], it is expected that a similar behavior would also be shown for pH-dependency of hydrodynamic radius as that observed in UV–Vis spectra (Fig. 4); hence, pH study while using DLS is not reported here. Further examination of Fig. 6 reflects that in addition to a similar hydrodynamic-temperature profile the average size of both hybrid samples (REA and RGA) is different. This difference is due to the difference in their overall chemical composition. Relatively larger hydrodynamic size was noted for sample RGA as compared to REA sample; this is due to higher NIPAAm ratio in sample RGA than REA. Higher amount of NIPAAm means improved hydrophilicity of gel particles solution and hence more hydrated water is being absorbed by the gel surface which in turn causes to increase the size of the particles.

Scanning Electron Microscopy (SEM)

SEM was employed in order to get more information about the growth of ZnO nanoparticles in polymeric microgel and/or growth of polymeric network around the ZnO nanoparticle core and the effect of hybridization on the surface morphology of individual moieties. Figure 7 shows some representative SEM images of pure microgels, ZnO NPs and ZnO loaded hybrid microgels. Before SEM, all samples were centrifuged, dried and then powdered. An obvious difference between the surface morphology of non-hybrid microgels, bare ZnO NPs and ZnO-(PNIAAm-CS-PAA) hybrid samples was seen in the SEM images; this is an indication of the successful fabrication of ZnO NPs inside the microgel network [21]. Furthermore, the change in various other physicochemical properties of both neat and hybrid materials, investigated by the other techniques as mentioned above, also support SEM results. It can be seen further that virgin ZnO NPs synthesized were not of the identical size throughout. The decoration of the cross-linked microgel globules and ZnO NPs was achieved by the firm contact between the side amine groups of the chitosan and ZnO particles may also incorporate within the spaces between the microgel chains.

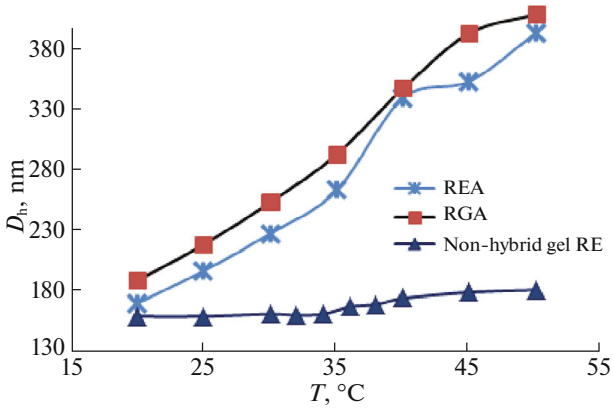

Fig. 6. Typical plots of hydrodynamic diameter (D_h) as a function of temperature of non-hybrid and ZnO loaded PNIPAAm-CS-PAA hybrid microgel samples at pH 4.

Thermogravimetric Analysis of Microgels

Thermogravimetric analysis (TGA) of the pure and hybrid microgel samples provides information regarding the thermal stability/decomposition and also about the thermo-kinetic behavior of the solid gel samples [33]. Figure 8 shows the graph between the weight losses (in mg) as a function of temperature in the range from 20–600°C for the representative non-hybrid and ZnO loaded PNIPAAm-CS-PAA hybrid microgel samples. In the temperature range of 40 to 170°C all the samples (RE, REA, RGA) show less prominent loss in their weight which is due to removal of water associated in the polymer matrix of the samples while no degradation was observed in this range of temperature. But as the temperature increases ($T > 170$°C) an obvious loss in weight was observed. This loss in weight continuous till the temperature reaches 415°C. This loss in weight can be due to the degradation of the side chains or low molecular weight chains of polymeric gels, while above this temperature the central chains/networks of polymeric gel started to degrade. A brief investigation shows that two temperature-level stages of thermal decomposition occurred in the ranges 40–140 and 250–460°C, which are due to water evaporation and thermal degradation of microgels, respectively. However, it can further be seen that complete degradation may occur at some temperature above 600°C. Results show that all the representative thermograms are typical of polymeric materials and are different from those of the crystalline materials. The overall phase of the microgels is changing from solid to rubbery phase and then to molten state and finally degraded (at $T >$ 600°C). The TG curves of the pure microgel (RE) are placed below the TG curves of ZnO-(PNIPAAm-CS-PAA) hybrid gel (REA and RGA). The difference in the overall thermograms of these samples is due to the difference in their chemical composition, especially, the effect of NIPAM content and hybridization with ZnO particles. Also the present results follow similar pattern as was observed in our previous work on pH-

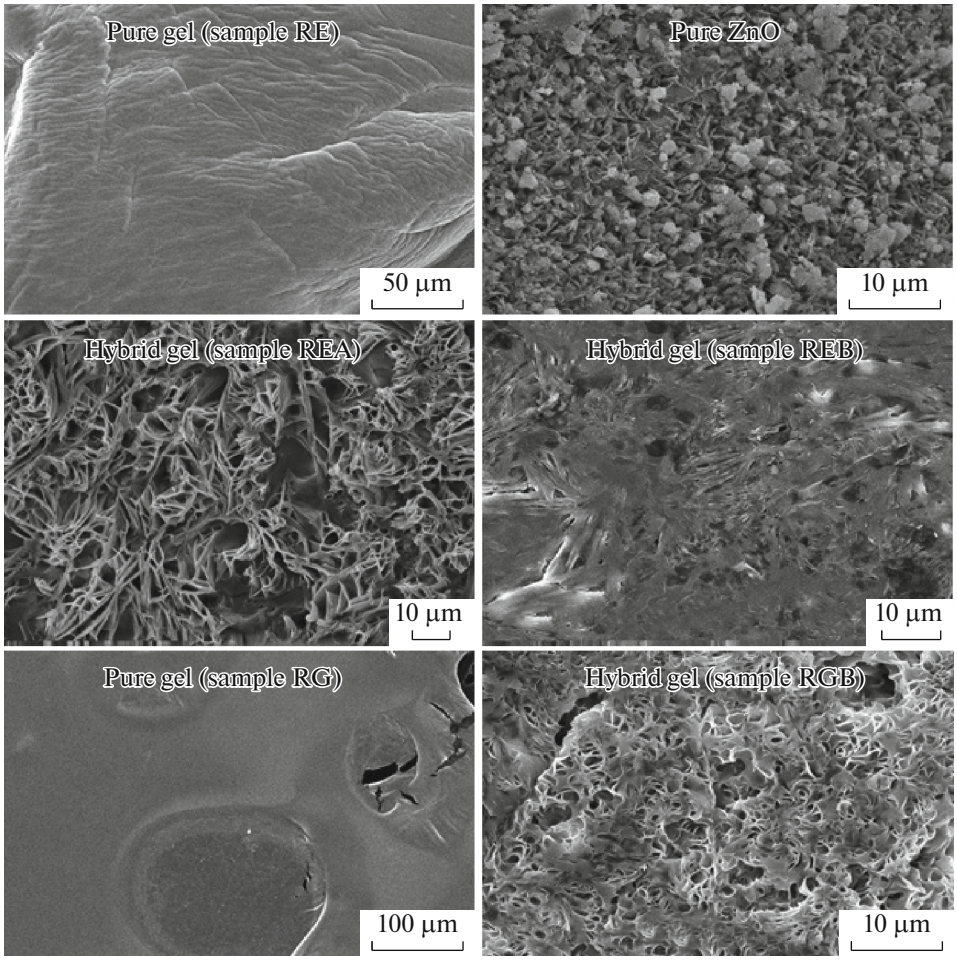

Fig. 7. Representative SEM images of pure microgels, ZnO NPs and ZnO loaded hybrid microgels.

responsive hydrogels [33], however, the difference in both cases is due to the difference in chemical composition. It can be seen that addition of ZnO to the polymeric gel leads not only to the thermal stability of the polymer gels but also to some changes in the phase transitional behavior. It is also reflected that the interactions of ZnO and PNIPAAm-CS-PAA based polymeric gels be of the physicochemical nature. Furthermore, the NIPAM content is high in sample RGA which makes it more sensitive to temperature as compared to sample REA, which is clear from the first step of the thermogram, where there is loss of free water from the microgel.

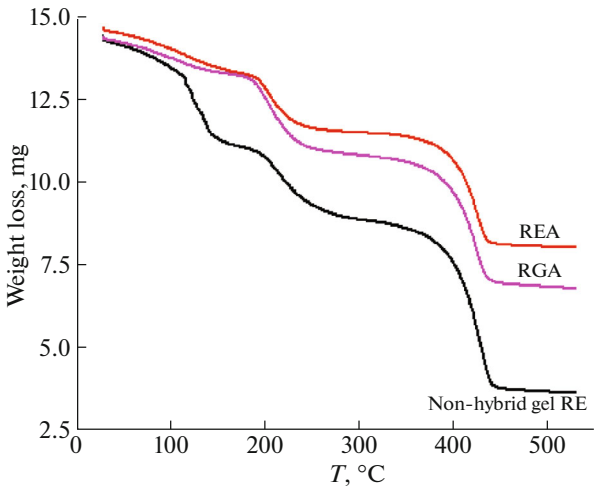

Fig. 8. Representative TGA plots for the thermal behavior of non-hybrid and ZnO loaded PNIPAAm-CS-PAA hybrid microgel samples as a function of temperature.

CONCLUSIONS

In the light of overall results, it is concluded that preparation and fabrication of pure microgels, ZnO nanostructured and ZnO-loaded hybrid pH/temperature responsive microgels were achieved successfully. The fabricated materials were characterized using UV–Vis, FTIR, SEM, DLS, and TGA. Presence of the characteristic absorption bands related to the vibration of ZnO in the hybrid gel samples was confirmed by FTIR an UV–Vis spectra. An increase in the absorbance of SPR (λ = 365–366 nm) of the hybrid microgels with increase in temperature as well as pH of the medium indicates an increase in the size

of hybrid materials which was also confirmed from results of DLS studies (hydrodynamic diameter). Changes in various physiochemical properties of the hybrid microgels upon changing the temperature/pH of solutions reflected the stimuli-sensitive behavior of the fabricated microgels. TGA results showed that the chemical composition, especially, the effect of NIPAM content and hybridization with ZnO particles affected the thermal behavior of these microgels. Likewise, the addition of ZnO to the polymeric gel leads not only to the thermal stability of the polymer gels but also to some changes in the phase transitional behavior. It was established that the hybrid microgel possess the combined features of integrated components to provide new materials with enhanced desirable properties; and such properties can be further adjusted by simple physical approaches while changing the quality and quantity of the stimuli. Further, this work also added some additional information to the field of polymer/inorganic hybrid nano-composites. It is also concluded that the decoration of the cross-linked microgel globules with ZnO NPs can be attained by the firm contact between the side amine groups of chitosan and the incorporation of inorganic particles within the spaces between the microgel chains/network.

REFERENCESW

1. A. S. Hoffman and P. S. Stayton, Prog. Polym. Sci. **32**, 922 (2002).
2. M. Motornov, Y. Roiter, I. Tokarev and S. Minko, Prog. Polym. Sci. **35**, 174 (2010).
3. M. Sirousazar, M. Forough, K. Farhadi, Y. Shaabani, and R. Molaei, in *Advanced Healthcare Materials,* Ed. by A. Tiwari (Wiley, Hoboken, NJ, 2014), p. 295.
4. A. Khan, U. Rehmat, L. A. Shah, and M. Usman, Russ. J. Phys. Chem. A **94**, 1503 (2020).
5. A. Khan, M. B. H. Othman, B. P. Chang, and H. M. Akil, Iran. Polym. J. **24**, 317 (2015).
6. K. Y. Lee, Macromol. Res. **15**, 195 (2007).
7. C. F. Lee, C. J. Wen, C. L. Lin, and W. Y. Chiu, J. Polym. Sci. Pol. Chem. **42**, 3029 (2004).
8. S. Y. Kim, M. Cho, and S. J. Kim, J. Appl. Polym. Sci. **78**, 1381 (2000).
9. R. Begum, K. Naseem, E. Ahmad, A. Sharif, and Z. H. Farooqi, Colloids Surf., A **511**, 17 (2016).
10. Z. H. Farooqi, K. Naseem, A. Ijaz, and R. Begum, J. Polym. Eng. **36**, 87 (2016).
11. T. U. Rehman, S. Bibi, M. Khan, I. Ali, L. A. Shah, A. Khan, and M. Ateeq, RSC Adv. **9**, 40051 (2019).
12. L. A. Shah, M. Syed, and M. Siddiq, Mater. Sci. - Poland **35**, 651 (2017).
13. Z. H. Farooqi, R. Begum, K. Naseem, U. Rubab, M. Usman, A. Khan, and A. Ijaz, Russ. J. Phys. Chem. A **90**, 2600 (2016).
14. S. Bai, C. Wu, K. Gawlitza, R. V. Klitzing, M. B. Ansorge-Schumacher, and D. Wang, Langmuir **26**, 12980 (2010).
15. D. Sivakumaran, D. Maitland, and T. Hoare, Biomacromolecules **12**, 4112 (2011).
16. A. C. Brown, S. E. Stabenfeldt, B. Ahn, R. T. Hannan, K. S. Dhada, E. S. Herman, V. Stefanelli, N. Guzzetta, A. Alexeev, and W. A. Lam, Nat. Mater. **13**, 1108 (2014).
17. X. Zhou, Y. Zhou, J. Nie, Z. Ji, J. Xu, X. Zhang, and B. Du, ACS Appl. Mater. Interfaces **6**, 4498 (2014).
18. R. Begum, Z. H. Farooqi, and S. R. Khan, Int. J. Polym. Mater. **65**, 841 (2016).
19. S. Wu, J. Dzubiella, J. Kaiser, M. Drechsler, X. Guo, M. Ballauff, and Y. Lu, Angew. Chem. Int. Ed. **51**, 2229 (2012).
20. A. H. Battez, R. González, J. Viesca, J. Fernández, J. D. Fernández, A. Machado, R. Chou, and J. Riba, Wear **265**, 422 (2008).
21. M. Humayun, A. Khan, A. Zada, M. Khan, M. N. Qureshi, and Z. Hussain, J. Chem. Soc. Pakist. **36**, 639 (2014).
22. D. Segets, J. Gradl, R. K. Taylor, V. Vassilev, and W. Peukert, ACS Nano **3**, 1703 (2009).
23. M. Chaari and A. Matoussi, Phys. B (Amsterdam, Neth.) **407**, 3441 (2012).
24. B. Ludi and M. Niederberger, Dalton Trans. **42**, 12554 (2013).
25. L. A. Shah, J. Mol. Liq. **288**, 111045 (2019).
26. S. Z. M. Rasib, H. M. Akil, A. Khan, and Z. A. A. Hamid, Int. J. Biol. Macromol. **128**, 531 (2019).
27. A. Khan, M. Sajjad, E. Khan, H. M. Akil, L. A. Shah, and Z. H. Farooqi, J. Polym. Res. **24**, 170 (2017).
28. M. S. Khan, G. T. Khan, A. Khan, and A. Shakoor, J. Chem. Soc. Pakist. **36**, 305 (2014).
29. R. Begum, Z. H. Farooqi, K. Naseem, F. Ali, M. Batool, J. Xiao, and A. Irfan, Crit. Rev. Anal. Chem. **48**, 503 (2018).
30. A. Khan, Colloid Interface Sci. **313**, 697 (2007).
31. J. M. Giussi, M. I. Velasco, G. S. Longo, R. H. Acosta, and O. Azzaroni, Soft Matter **11**, 8879 (2015).
32. Z. H. Farooqi, N. Tariq, R. Begum, S. R. Khan, Z. Iqbal, and A. Khan, Turk. J. Chem. **39**, 576 (2015).
33. M. B. H. Othman, H. M. Akil, S. Z. M. Rasib, A. Khan, and Z. Ahmad, Ind. Crops Prod. **66**, 178 (2015).